Insight into the Role of Additives in Catalytic Synthesis of Cyclohexylamine from Nitrobenzene

Xuefeng Li‡, Zhe Wang‡, Shanjun Mao, Yiqing Chen, Minghui Tang, Haoran Li, Yong Wang**

ABSTRACT Cyclohexylamine is a versatile intermediate in various chemical industries, which can be expediently synthesized via hydrogenation of aniline or nitrobenzene. However, such processes always suffer from side reactions. Many reports have found that specific additives can suppress the formation of side products, but the mechanism is still not clear. In this work, results suggest that it is the hydroxide ion of alkali metal hydroxides, rather than the cations, which plays a key role in suppressing the side reactions on supported Ru-based catalysts. With the assistance of LiOH, the selectivity toward cyclohexylamine increased from 85.4% to 100%. Side products, such as dicyclohexylamine, cyclohexanol and N-isopropyl cyclohexylamine could no longer be detected. Theoretical calculations further disclosed that addition of alkali metal hydroxides inhibited the dissociation of enamine and decreased the adsorption energy of cyclohexylamine, which might be the reasons for a better selectivity. However, the addition of alkali metal hydroxides reduced the activity of nitrobenzene hydrogenation by unfolding the condensation reaction route. To recover or even further enhance the catalytic performance, a second metal component was introduced and the resultant RuNi/AC exhibited a significant improvement in activity compared with Ru/AC.

KEYWORDS cyclohexylamine, nitrobenzene, hydrogenation, heterogeneous catalysis, basicity, bimetallic catalysts

Introduction

The hydrogenation of nitroarenes to primary cycloaliphatic amines is a reaction of great academic and commercial importance for many processes in pharmaceutical chemistry and petroleum industry.[1,2] For instance, most studies concerning nitroarenes hydrogenation have used nitrobenzene (NB) as the model aromatic feed molecule. Indeed, cyclohexylamine (CHA) obtained from the complete hydrogenation of NB is a high-value intermediate used in the production of polymers, medicines and fine chemicals.[3,4] One-pot catalytic hydrogenation of NB to CHA, combining multiple chemical transformations without separation and purification, provides a much greener pathway in view of cost saving. However, the direct synthesis of CHA from NB suffers from the significant challenges in catalysts design, which requires one-pot hydrogenation of the nitro and aromatic ring with high activity and selectivity.

As illustrated in Scheme 1, two steps are often required to transform NB to CHA. The first step involves the reduction of the nitro group to aniline (AN). According to previous researches,[5-9] there are two possible reaction pathways in this step, i.e. the direct route (upside pathway in Scheme 1) and condensation route (bottom pathway in Scheme 1). In general, the reaction rate for the condensation route is slower than that for the direct one, and no selectivity issue occurs in this step. In fact, it is the following reduction of the aromatic ring that determines the selectivity of the whole hydrogenation. However, it always suffers from side reactions. The main side products are dicyclohexylamine (DCHA, from condensation of imine and CHA) and cyclohexanol (from condensation of enamine and water).[10] At relatively high temperature (above 160-170 ^{o}C), DCHA can also be generated via the condensation of two molecules of CHA. Therefore, many efforts have been devoted to improving the selectivity toward CHA in the second step.

It has been found that the addition of ammonia suppressed the formation of secondary amines during the hydrogenation of AN as early as 1940.[11] However, the presence of ammonia poisoned the catalyst with a great activity loss. Later, alkali hydroxides were found not only to be effective in suppressing the formation of the side products but also to have a promotional effect on the aromatic amines hydrogenation.[12,13] Shigeo Nishimura et al. proposed that alkali hydroxides possibly prevented a longer stay of CHA on the catalyst surface and thus inhibited the condensation between imine and CHA,[13] but no further experimental evidence was given. Interestingly, the addition of alkali metal nitrites was also found to be effective in suppressing the formation of secondary amines.[14] Thomas E. Müller's group then proposed that the nitro promoter and amine groups formed a hydrogen-bonded adduct on the catalyst surface, which could probably stabilize the enamine and thus prevent the condensation reactions.[15,16] Besides the alkali metal hydroxides and nitrites, using strong basic metal oxides as support could also result in a high selectivity to primary amines in the vapor phase hydrogenation of aniline.[17]

As stated above, although previous work suggests that alkali metal hydroxides and nitrites are efficient additives for suppressing the formation of secondary amines, the reasons are still unclear. What's more, the phenomenon with two dissimilar species exhibiting the same effect is rather confusing. Therefore, the emphasis in the present work was placed on investigating the influences of additives on the hydrogenation of NB to CHA. In addition, to compensate the activity loss induced by additives, or to achieve an even better catalytic performance, a series of bimetallic catalysts, RuM/AC (M=Fe, Co, Ni, Cu and In), were prepared.

Results and Discussion

Among various hydrogenation catalysts, supported Ru-based catalysts are widely used in the hydrogenation of NB to CHA, due to their excellent performance.[16,18] Therefore, the hydrogenation of NB was carried out over supported Ru/AC in initial catalytic experiments. Since the free electron pair on the nitrogen atom of amines causes a strong adsorption on the metallic catalyst, CHA cannot desorb from the active sites easily and then suffers from condensation reactions.[13,17] As a result, the side product DCHA was inevitably formed during the hydrogenation of NB to CHA without addition of additives (11.6% of DCHA, Table 1, entry 1). In order to investigate the influences of additives on selectivity of CHA, various types of alkali metal salts were added into the reactor. Table 1 showed that addition of alkali metal hydroxides, nitrates

Advanced Materials and Catalysis Group, Institute of Catalysis, Zhejiang University, Hangzhou 310028, P. R. China
E-mail: chemwy@zju.edu.cn

This article has been accepted for publication and undergone full peer review but has not been through the copyediting, typesetting, pagination and proofreading process, which may lead to differences between this version and the Version of Record. Please cite this article as doi: 10.1002/cjoc.201800380

Scheme 1. Reaction routes for the hydrogenation of nitrobenzene to cyclohexylamine.

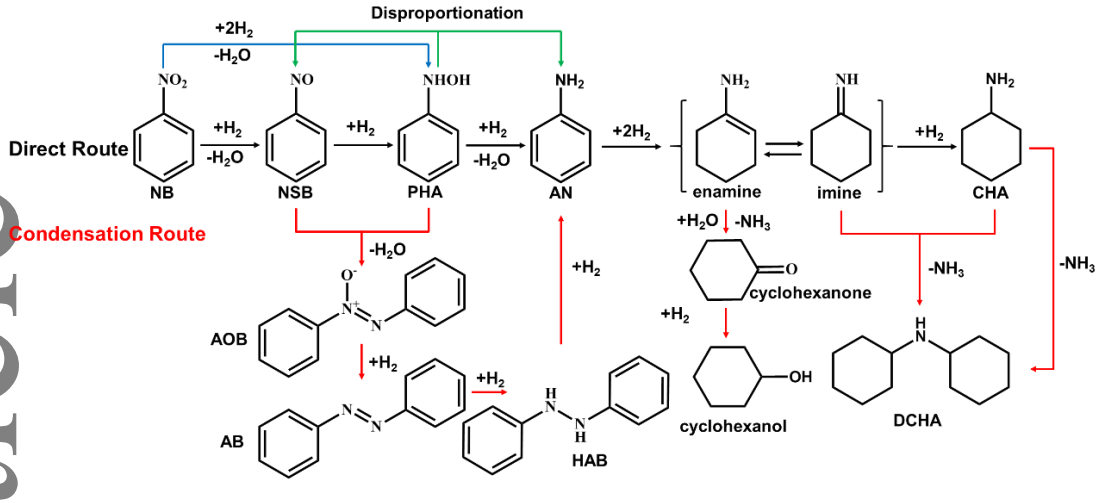

NB: nitrobenzene, NSB: nitrosobenzene, PHA: phenylhydroxylamine, AOB: azoxybenzene, AB: azobenzene, HAB: hydrazobenzene, AN: aniline, CHA: cyclohexylamine, DCHA: dicyclohexylamine.

Table 1. Effects of additives on NB hydrogenation[a]

Entry	Additives	Conv.%	Sel.%				pH[a]	pH[b]
			AN	CHA	DCHA	Others		
1	None	100		85.4	11.6	3.0		
2	LiOH	100		100				
3[b]	NaOH	100		100				
4	KOH	100		100				
5	RbOH	100		100				
6[b]	$LiNO_3$	100		100			13.08	12.09
7	$NaNO_3$	100		100			13.10	12.27
8	$NaNO_2$	100		100			13.18	12.24
9	KNO_3	100		100			13.31	12.29
10	$Na_3PO_4•12H_2O$	100		91.9	4.3	3.9	12.89	12.62
11	$Na_2HPO_4•12H_2O$	100		88.6	8.3	3.1		
12	$NaH_2PO_4•2H_2O$	100		83.2	9.7	7.1		
13	$Na_2B_4O_7•10H_2O$	100		94.6	4.4	1.0	11.11	11.08
14	$NaAlO_2$	100		93.9	3.2	3.0	12.28	12.47
15	NaCl	100		87.3	10.6	2.1	11.81	12.05
16	Na_2SO_4	100		86.6	10.4	3.0	12.04	12.09
17	K_2SO_4	100		84.7	12.1	3.2	12.05	12.12
18[b]	$NH_3•H_2O$	100		84.5	8.9	6.6		
19[b]	0.2 mL $NH_3•H_2O$	100		91.7	2.3	6.0		
20[b]	0.5 mL $NH_3•H_2O$	100		89.3	1.7	9.0		

[a]Conditions: 20 mg catalyst, 1 mmol NB, 0.1 mmol additive, internal standard: isooctane, 5 mL IPA, 90 °C, 6 MPa H_2, 50 min.

[b]Substrate was reduced to 0.5 mmol and/or reaction time was prolonged.

pH[a]: The pH values of the reaction solution after the hydrogenation (dilute with same volume of deionized water).

pH[b]: The pH values of the solution prepared through adding additives and corresponding products into mixed liquid of IPA and deionized water (volume ratio=1:1).

and nitrites was more effective in suppressing the formation of side products compared with other metal salts and a nearly 100%

[a] Department, Institution, Address 1
E-mail:
[b] Department, Institution, Address 2
E-mail:
[c] Department, Institution, Address 3
E-mail:

selectivity toward CHA was obtained (Table 1, entry 2-9). Addition of weak alkalis, such as Na_3PO_4, $Na_2B_4O_7$ and $NaAlO_2$, showed moderate suppression on side reactions. Especially, the suppression effect weakened along with the decrease of alkalinity of Na_3PO_4, Na_2HPO_4 and NaH_2PO_4 (Table 1, entry 10-12). However, no significant influence on the selectivity was observed by the addition of such neutral metal salts as NaCl, Na_2SO_4 and K_2SO_4 (Table 1, entry 15-17). For example, NaCl led to a yield of 87.3% for CHA and 10.6% for DCHA, which is almost in the same level as the blank experiment (Table 1, entry 1), indicating the inertness of NaCl in this hydrogenation reaction.

The above results suggest that the alkalinity of additives has a significant effect on products distribution. Then what causes the difference between the nitrates, nitrites and other neutral metal salts. It was reported that nitrates and nitrites can be reduced at ambient temperature and atmospheric H_2 pressure in a fixed-bed reactor, leading to the formation of the hydroxide ion.[19-21] The pH of the reaction solution before and after the hydrogenation were then measured. As shown in Table 1, the pH values of the solution including alkali metal nitrates and nitrites increased obviously after the hydrogenation (Table 1, entry 6-9). For example, the pH value of $LiNO_3$ solution increased from 12.09 to 13.08 after the hydrogenation, indicating the reduction of NO_3^- and formation of hydroxide ion. However, for other metal salts, only minor pH changes were observed after the hydrogenation (Table 1, entry 10, 13-17).

Conclusively, among various types of additives, alkali metal hydroxides are effective in suppressing side reactions, but other metal salts (alkali metal sulfates, phosphates, halides, etc.) are not. Therefore, it seems that it is the hydroxide ion that play a key role in affecting the products distribution, rather than the metal cations. To confirm our deduction, the hydrogenation reactions were then performed in the presence of ammonium hydroxide. As shown in Table 1, entry 18, addition of $NH_3 \bullet H_2O$ showed moderate suppression on the formation of DCHA (8.9% of DCHA). The selectivity toward DCHA further decreased from 8.9 to 1.7% when increasing the dosage of ammonia aqueous solution form 42 μL to 0.5 mL, indicating that the hydroxide ion indeed plays a key role in suppressing the formation of DCHA. It should be pointed out that the increase of other side products is due to the presence of water, which will be discussed below.

In order to get detailed information about the influences of alkali metal hydroxides, the time-concentration profiles of the substrate and products were illustrated with LiOH as a representative in the following study. As shown in Figure 1 A, in absence of LiOH, NB directly converted to AN at the early stage of the reaction. No intermediates, such as nitrosobenzene (NSB) and azoxybenzene, were detected during the conversion process, indicating that the nitro group hydrogenation probably followed the direct route (Scheme 1). The hydrogenation of AN began when NB was almost fully consumed, accompanied with the formation of side products, such as DCHA and cyclohexanol (Figure 1 A). However, when LiOH was added, the profile of the reaction changed significantly. As illustrated in Figure 1 B, intermediates along with the condensation route, such as azoxybenzene and azobenzene were detected during the hydrogenation of the nitro group. Accordingly, the hydrogenation rate of the nitro group slowed down greatly. The time to achieve 90% conversion (for NB) increased from 35 to 60 min, i.e. the average activity reduced by nearly 70%. However, in contrast to the first step, modification with LiOH significantly suppressed side reactions during the hydrogenation of the aromatic ring (Figure 1 B) and distinctly accelerated the rate of aromatic ring hydrogenation (Table 2). In fact, a selectivity of 100% toward CHA was achieved.

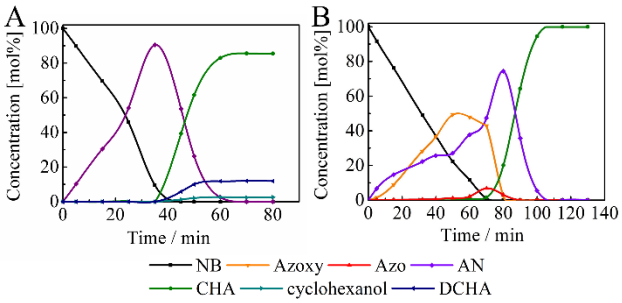

Figure 1. NB reaction profile over Ru/AC in the absence (A) or presence (B) of LiOH. Conditions: catalyst 60 mg, 4.5 mmol NB, 15 mL IPA, pressurized to 7.2 MPa with H_2 after heating the reactor to 90 °C.

Table 2. The hydrogenation of AN on Ru/AC

Additive	Conv.%	Sel.%		
		CHA	DCHA	Others
None	76.8	80.6	15.1	4.3
LiOH	100	100	-	-

Conditions: catalyst 20 mg, 1.5 mmol AN, 5 mL IPA, pressurized to 7.2 MPa with H_2 after heating the reactor to 90 °C, reaction time was 10 min.

Table 3. Effect of water on the distribution of products[a]

Entry	Water	Sel.%			
		CHA	DCHA	Cyclohexanol	IP-CHA
1[b]	None	85.4	11.6	2.7	0.3
2	None	82.2	15.1	0.7	2.0
3	0.1 mL	81.3	14.9	2.5	1.3
4	1.0 mL	87.9	7.8	4.2	0
5	5.0 mL	78.7	5.8	15.5	0
6[c]	None	71.0	29.0	0	0

[a]Conditions: catalyst 20 mg, 1 mmol AN, 5 mL IPA, 90 oC, 6 MPa H2, 50 min.

[b]Substrate was NB.

[c]THF used as solvent, the reaction system was dealt with CaH2 to remove any possible water, and reaction time was 90 min.

As can be seen in Table 2, besides DCHA, side products such as cyclohexanol and N-isopropyl CHA (IP-CHA) were also detected during the hydrogenation of AN in absence of LiOH, probably due to the reaction of intermediates (enamine or imine) with water and IPA, respectively.[10,22] This could be clarified by the experimental results from Table 3. As shown, when NB was used as substrate, 2.7% selectivity toward cyclohexanol was obtained. However, when replacing NB by AN, i.e. removing the water from the hydrogenation of the nitro group, the selectivity toward cyclohexanol decreased to 0.7%. Such results indicate the amount of water in the reactor may well determine the selectivity of cyclohexanol. Therefore, we gradually increased the amount of water to 5.0 mL deliberately. As expected, the selectivity toward cyclohexanol rose from 0.7 to 15.5%. It should be noted that the remained tiny production of cyclohexanol even when AN was used as substrate, was mostly owed to the presence of unavoidable trace water in the reactor, which could be derived from solvent, reduction of RuO_x on the catalyst surface and condensation between IPA and intermediates. Then two controlled experiments were done to guarantee the removal of the left water. One is substituting tetrahydrofuran (THF) for IPA. The other is treating the reaction solution with CaH_2 (detailed processes were described in Supporting Information, Table S1). As

shown in Table 3, entry 6, when water was removed completely, cyclohexanol could not be detected any more. These results clearly demonstrate that cyclohexanol is generated from the condensation of intermediates and water. It should be pointed out that with the increase of cyclohexanol, the selectivity toward DCHA decreased from 15.1 to 5.8% (Table 3, entry 2-5), which could be attributed to the competition between the two side reactions.

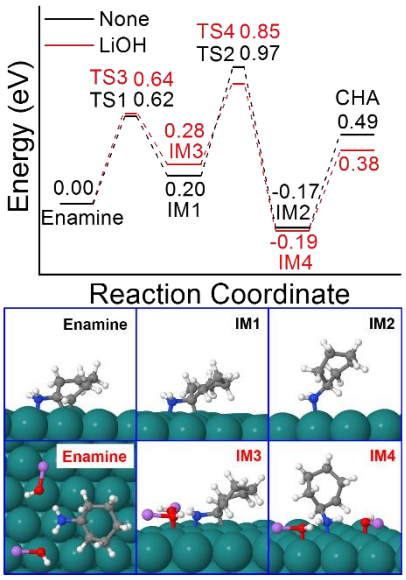

Figure 2. The energy profile for the conversion of enamine to CHA on the Ru catalyst. None: no additive; LiOH: with LiOH addition. Color code: dark green is Ru; gray is carbon; blue is nitrogen; purple is Li; light white is hydrogen.

To deeply investigate the promotional effects of LiOH on the second step, i.e. hydrogenation of AN, theoretical calculations were performed. According to Scheme 1, the conversion of enamine is fatal to the selectivity. Hence, our calculations start from enamine. The adsorption energy of enamine on the clean surface of Ru (0001) is -0.76 eV (negative value means an exothermic process), indicating a rather stable adsorption. When LiOH was considered, two LiOH units were added to Ru (0001) owing to the two hydrogen bonds between the amino group and LiOH. The adsorption energy of the two LiOH units alone on Ru (0001) is rather large (-3.35 eV), which implies the favorable locating of LiOH on Ru. Interestingly, the adsorption energy of enamine changes little (-0.77 eV) when LiOH was considered. The reason may be the weakening of the C-Ru bond caused by the structure re-optimation.

As reaction proceeds, enamine may tautomerize to imine and then convert to side products as DCHA by dissociating one H atom of the amino group to the Ru surface firstly. This step is calculated to be energy rather favorable (-0.29 eV). However, when LiOH is added, this step is totally inhibited (no stable dissociation structures are founded) by the steric hindrance from LiOH. Owing to which, the selectivity is improved.

As to the main route to the desirable product, the first H addition step of enamine was almost not affected by LiOH as seen in Figure 2. However, situation for the second H addition, i.e. the rate determination step for enamine hydrogenation, is another case. This step is promoted in both thermodynamics (0.1 eV) and kinetics (0.2 eV) by LiOH, in accordance with the experimental results. In addition, the decrease of the desorption energy for the product (from 0.66 to 0.57 eV) with LiOH, which means more active sites are released, may be another factor for the enhanced activity as discussed earlier.

Table 4. Comparison of the catalytic performance over different bimetallic catalysts[a]

Cat.	Conv.%	Sel.%		
		AOB+AB	AN	CHA
Ru/AC	35.6	15.8	84.2	0
RuFe/AC	56.2	37.9	62.1	0
RuCo/AC	67.5	70.5	29.5	0
RuNi/AC	100	0	23.9	76.1
RuCu/AC	73.4	6.2	93.9	0
RuIn/AC[b]	100	0	36.3	51.0
Ni/AC	39.2	96.5	3.5	0
Ru/AC+Ni/AC[c]	68.5	45.1	54.9	0
Ru^Ni/AC	100	58.0	42.0	0

[a]Conditions: catalyst 20 mg, 1 mmol NB, 0.1 mmol LiOH, 5 mL IPA, 70 °C, 6 MPa H_2, 1 h.

[b]Other products are 11.6% of DCHA and 1.1% of cyclohexanol.

[c]The physical mixture of Ru/AC and Ni/AC.

As shown in Figure 1 B and Table 2, although side reactions were greatly suppressed by addition of alkali additives, the overall catalytic activity also decreased with a low-rate condensation route being opened for hydrogenation of the nitro group. Previous reports have demonstrated that introducing cheap metals (such as Fe, Co, Ni and Cu) into noble metals (such as Pt, Ru, Rh and Re) can improve the catalytic performance of hydrodeoxygenation reactions due to their synergetic effects.[23-28] Since the hydrogenation of the nitro group also involves a deoxygenation process, it might be facilitated by introducing a second suitable metal component in this reaction. Based on this point, a series of bimetallic catalysts were developed by a co-impregnation method. As can be seen from Table 4, under given reaction conditions, introducing a second metal component into Ru catalysts indeed improved the activity to various extent. The conversion of NB improved from 35.6% to 56.2, 67.5 and 73.4% by introducing Fe, Co and Cu respectively. Introduction of In and Ni gave a much better catalytic activity by yielding CHA of 51.0 and 76.1%, respectively. Thus, among RuM/AC catalysts (M=Fe, Co, Ni, Cu and In), RuNi/AC gave the best catalytic performance (the time-concentration profiles can be seen from Figure S3).

To gain insight into synergistic effects of Ru and Ni, some controlled experiments were also performed. As shown in Table 4, entry 8, the physical mixture of Ru/AC and Ni/AC gave only 68.5% conversion of NB, far less efficient than RuNi/AC, indicating that the enhanced performance of RuNi/AC is mainly ascribed to the interaction between Ru and Ni, not the aggregate activity of two metals. Additionally, Ru^Ni/AC, prepared through a consecutive impregnation method, also showed a lower catalytic performance in comparison with RuNi/AC (Table 4, entry 9), suggesting the process of preparation has a significant effect on catalytic performance.

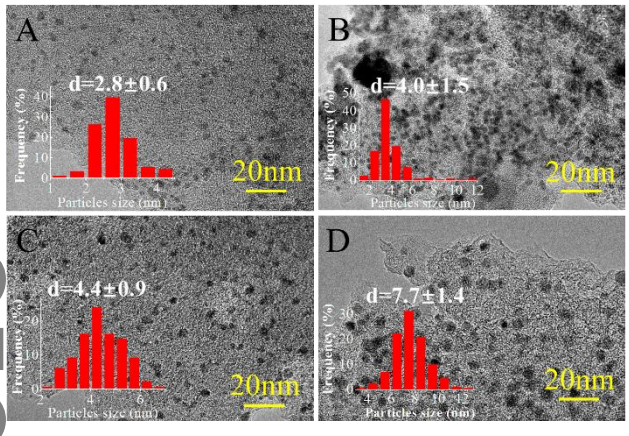

Figure 3. HRTEM images and particle size distribution of (A) RuNi/AC, (B) Ru^Ni/AC, (C) Ru/AC, (D) Ni/AC.

To get further insight into supported bimetallic catalysts, various characterizations were conducted. Figure 3 shows a typical set of HRTEM images for the RuNi/AC, Ru^Ni/AC, Ru/AC and Ni/AC samples. For RuNi/AC, the bimetallic nanoparticles, which can be demonstrated through EDX line-scan profile (Figure S4 A), were well dispersed on AC support, with an average size of 2.8 nm and a narrow distribution (Figure 3 A), while obvious agglomerations of metal particles (4.0 nm) were observed in the Ru^Ni/AC (Figure 3 B). For monometallic Ru/AC and Ni/AC, the average size of metal particles was 4.4 and 7.7 nm respectively (Figure 3 C and 3 D), larger than bimetallic nanoparticles. These results from HRTEM analysis suggest that the small mean metal particles of RuNi/AC might be a factor for the enhanced catalytic performance. However, it should be noticed that Ru^Ni/AC had a similar mean metal particles size to Ru/AC, but showed a better performance (Table 4, entry 1, 8 and 9), indicating that the better dispersion is not the only reason for the outstanding performance of bimetallic catalysts.

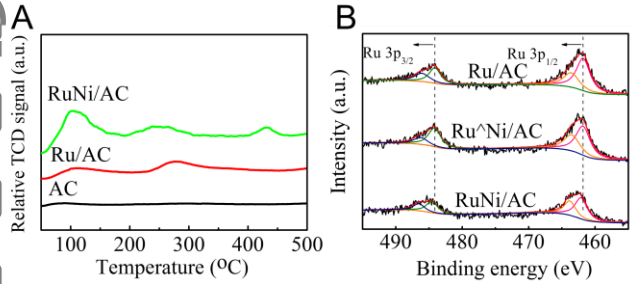

Figure 4. NH_3-TPD profiles (A) and XPS spectra of Ru 3p (B) of various supported catalysts.

As mentioned above, the hydrogenation of the nitro group involves a deoxygenation process or dehydration process,[29] thus the acidity of catalysts possibly has influences on catalytic performance.[30-32] NH_3-TPD analysis was then conducted to determine the acidity of Ru/AC and RuNi/AC. As shown in Figure 4 A, Ru/AC presented two ammonia desorption peaks at about 105 and 275 °C. However, the situation changed when Ru nanoparticles were alloyed with Ni, three ammonia desorption peaks appeared at about 100, 250 and 430 °C on RuNi/AC, respectively. The newly appeared peak at 430 °C can be attributed to the strong acid sites on NiO (The chemical state of Ni can be seen in the XPS analysis below).[33-34] Obviously, compared with Ru/AC, both the acid strength and the amounts of acid sites increased after introducing Ni, which might be another factor for the improved activity.

Table 5. Binding energy (eV) of Ru 3p obtained from curve-fitted XPS spectra for different catalysts

Catalyst	Ru $3p_{3/2}$, eV		Ru $3p_{1/2}$, eV		Relative percentage, %
	Ru^{n+}	Ru^0	Ru^{n+}	Ru^0	Ru^0/Ru^{n+}
Ru/AC	463.6	461.8	486.0	484.1	64/36
Ru^Ni/AC	463.5	461.8	486.2	484.1	65/35
RuNi/AC	463.8	462.1	486.5	484.5	61/39

XPS analysis was further employed to examine the electronic structures of the bimetallic catalysts. The surface Ni is mainly oxidized (Figure S6). Ru 3p peaks were used to determine the chemical state of Ru because Ru $3d_{3/2}$ peak overlaps with that of C 1s on the support.[35] As can be seen from Figure 4 B and Table 5, Ru^0/Ru^{n+} in these catalysts is almost in the same level. However, the binding energy of Ru 3p in RuNi/AC catalysts showed an obvious positive shift (0.2-0.5 eV) with respect to Ru/AC and Ru^Ni/AC, indicating metallic Ru become more electron-deficient. This may also be helpful since it has been reported electron-deficient Ru are efficient for hydrogenation of NB due to the easy desorption of AN.[18,36,37]

Conclusions

The present work has investigated the influences of additives on the hydrogenation of NB over supported Ru-based catalysts. 100% selectivity toward CHA was achieved by addition of alkali metal hydroxides, nitrites and nitrates. Results suggest that the suppression on side reactions derived from different additives is actually attributed to effects of the hydroxide ion. Theoretical calculation further suggests that alkali metal hydroxides can lower the energy barrier for enamine hydrogenation and release more active sites by decreasing the adsorption energy of CHA, which is beneficial for the hydrogenation of the aromatic group. The easier desorption of CHA from the active sites, which prevents it from reacting with imine, and the suppression of enamine dissociation caused by alkali metal hydroxides may be the reasons for better selectivity. However, modification with alkali additives suppressed the hydrogenation of the nitro group. To compensate this activity loss, various bimetallic catalysts were prepared. The resultant RuNi/AC showed very high activity with a yield of CHA up to 76.1%, while Ru/AC gave only 35.6% conversion of NB.

Experimental

Chemicals. $RuCl_3$ (Ru, 50 wt%), LiOH (98%) and $LiNO_3$ (AR) were used as received from Aladdin Chemistry Co., Ltd. Isopropyl alcohol (AR), nitrobenzene (AR), aniline (AR), NaOH (AR), KOH (AR), and $NaNO_3$ (AR) were purchased from Sinopharm Chemical Reagent Co., Ltd. Commercial activated carbon (AC) was obtained from Jiangsu Liangyou Environmental Protection Technology Co. Ltd.

Preparation of Catalyst. The catalyst was prepared by the impregnation method.[35] In a typical process, 0.4 g AC was dispersed into deionized water (40 mL) in a beaker under magnetic stirring, and then 4 mL $RuCl_3$ aqueous solution (0.01 g/mL) was added into the beaker. The beaker and mixture were then heated in an oil bath at 60 °C with stirring to evaporate the water. The obtained black powder was reduced under the atmosphere of H_2 at 300 °C for 2 h with a heating rate of 10 °C /min. The obtained catalyst was denoted as Ru/AC.

RuM/AC (M=Fe, Co, Ni, Cu and In) was prepared as the same method expect a little difference. The amount of the second

metal was fixed at 1/1 by the weight ratio of the additive to Ru. Before reduction at 400 °C, the precursor was calcined at 300 °C (the heating rate = 10 °C/min) for 2.5 h in air. For comparison, a consecutive impregnation method was employed for the catalyst preparation. The support was first impregnation with $Ni(NO_3)_2•6H_2O$, dried, calcined at 300 °C for 2.5 h and was then impregnation with $RuCl_3$, dried, calcined at 300 °C for 2.5 h. After reduction, the catalyst Ru^Ni/AC was obtained.

Characterizations. HRTEM, STEM-HAADF and STEM-EDX (JEM-2100F) were carried out to observe the morphology, the particle size distribution and element distribution of the catalyst. Powder X-ray diffraction (XRD) patterns were conducted on a D/tex-Ultima TV wide angle X-ray diffractometer equipped with Cu Ka radiation (40 kV, 30 mA, 1.54 Å). X-ray photoelectron spectra (XPS) were recorded on an ESCALAB MARK II spherical analyzer using an aluminum-magnesium binode (Al 1486.6 eV, Mg 1253.6 eV) X-ray source. The binding energies were corrected with reference to C 1s line at 284.5 eV. Temperature programmed reduction (TPR) was performed on a quartz reactor connected to a thermal conductivity detector (TCD) under an atmosphere of 10% H_2/Ar from room temperature to 500 °C at a heating rate 10 °C/min. Temperature programmed desorption of ammonia (NH_3-TPD) was conducted to study the surface acidity of catalysts.

Catalytic Tests. All hydrogenation reactions were carried out in a 50 mL stainless steel autoclave equipped with a magnetic stirrer. In a typical process, the mixture of reactant, additive, internal standard (isooctane), solvent (isopropanol) and powder catalyst was introduced into the sealed autoclave. The autoclave was purged with H_2 three times to remove any remaining air and then pressurized to 6 MPa with H_2. The reactor was heated to reaction temperature and the reaction was allowed to proceed for a certain time. After completion of the reaction, the mixture was separated by centrifugation. The resulting solution was analyzed by GC-FID and the products were identified by GC-MS.

Computational Setup. The calculations are performed by using periodic, spin-polarized DFT as implemented in Vienna ab initio program package (VASP).[38,39] The electron-ion interactions are described by the projector augmented wave (PAW) method proposed by Blöchl[40] and implemented by Kresse.[41] RPBE functional[42] is used as exchange-correlation functional approximation. A plane wave basis set with an energy cutoff of 400 eV is used. A p (5×5) surpercell containing a four-layer slab with 100 atoms was modeled as catalyst and (0001) plane is considered as the active surface. a (2×2×1) k-point grid is used for the Brillouin zone sampling. The periodic condition is employed along the x and y direction. The vacuum space along the z direction was set to be 13 Å. The upper two layer atoms in the cell are allowed to relax during the structure optimization, while the bottom two layer atoms are fixed. The relaxation is stopped when the force residue on the atom is smaller than 0.02 eV/ Å. The transition states are calculated by using the climbing image nudged elastic band (CI-NEB) method.[43]

Supporting Information

The supporting information for this article is available on the WWW under https://doi.org/10.1002/cjoc.2018xxxxx.

Acknowledgement

Financial support from the National Natural Science Foundation of China (91534114, 21622308), the Key Program Supported by the Natural Science Foundation of Zhejiang Province, China (LZ18B060002) and the Fundamental Research Funds for the Central Universities (2017XZZX002-16) are greatly appreciated.

References

[1] Wei, Z. Z.; Wang, J.; Mao, S. J; Su, D. F; Jin, H. Y.; Wang, Y. H.; Xu, F.; Li, H. R.; Wang, Y. *ACS. Catal.* **2015**, 5, 4783-4789.
[2] Cao, Y. L.; Mao, S. J.; Li, M. M.; Chen, Y. Q.; Wang, Y. *ACS Catal.* **2017**, 7, 8090-8112.
[3] Narayanan, S.; Unnikrishnan, R.; Vishwanathan, V. *Appl. Catal. A* **1995**, *129*, 9.
[4] Chatterjee, M.; Sato, M.; Kawanami, H.; Ishizaka, T.; Yokoyama, T.; Suzuki, T. *Appl. Catal. A* **2011**, *396*, 186.
[5] Corma, A.; Concepcion, P.; Serna, P. *Angew. Chem. Int. Ed.* **2007**, *46*, 7266.
[6] Combita, D.; Concepción, P.; Corma, A. *J. Catal.* **2014**, *311*, 339.
[7] Zhang, L.; Jiang, J.; Shi, W.; Xia, S.; Ni, Z.; Xiao, X. *RSC Adv.* **2015**, *5*, 34319.
[8] Liu, W.; Zhang, L.; Yan, W.; Liu, X.; Yang, X.; Miao, S.; Wang, W.; Wang, A.; Zhang, T. *Chem. Sci.* **2016**, *7*, 5758.
[9] Liu, X.; Li, H.-Q.; Ye, S.; Liu, Y.-M.; He, H.-Y.; Cao, Y. *Angew. Chem. Int. Ed.* **2014**, *53*, 7624.
[10] Greenfield, H. *J. Org. Chem.* **1964**, *29*, 3082.
[11] Winans, C. F. *Ind. Eng. Chem.* **1940**, *32*, 1215.
[12] Nishimura, S.; Kono, Y.; Otsuki, Y.; Fukaya, Y. *Bull. Chem. Soc. Jpn.* **1971**, *44*, 240.
[13] Nishimura, S.; Shu, T.; Hara, T.; Takagi, Y. *Bull. Chem. Soc. Jpn.* **1966**, *39*, 329.
[14] Kim, H. S.; Seo, S. H.; Lee, H.; Lee, S. D.; Kwon, Y. S.; Lee, I. M. *J. Mol. Catal. A* **1998**, *132*, 267.
[15] Gebauer-Henke, E.; Tomkins, P.; Leitner, W.; Mueller, T. E. *Chemcatchem* **2014**, *6*, 2910.
[16] Tomkins, P.; Gebauer-Henke, E.; Leitner, W.; Müller, T. E. *ACS Catal.* **2014**, *5*, 203.
[17] Mink, G.; Horvath, L. *React. Kinet. Catal. Lett.* **1998**, *65*, 59.
[18] Leng, F.; Gerber, I. C.; Lecante, P.; Moldovan, S.; Girleanu, M.; Axet, M. R.; Serp, P. *ACS Catal.* **2016**, *6*, 6018.
[19] Trawczyński, J.; Gheek, P.; Okal, J.; Zawadzki, M.; Gomez, M. J. I. *Appl. Catal. A* **2011**, *409-410*, 39.
[20] Al Bahri, M.; Calvo, L.; Gilarranz, M. A.; Rodriguez, J. J.; Epron, F. *Appl. Catal. B* **2013**, *138*, 141.
[21] Brunet Espinosa, R.; Lefferts, L. *ACS Catal.* **2016**, *6*, 5432.
[22] Oh, S. G.; Mishra, V.; Cho, J. K.; Kim, B.-J.; Kim, H. S.; Suh, Y.-W.; Lee, H.; Park, H. S.; Kim, Y. J. *Catal. Commun.* **2014**, *43*, 79.
[23] Do, P. T. M.; Foster, A. J.; Chen, J.; Lobo, R. F. *Green Chem.* **2012**, *14*, 1388.
[24] Hensley, A. J. R.; Hong, Y.; Zhang, R.; Zhang, H.; Sun, J.; Wang, Y.; McEwen, J.-S. *ACS Catal.* **2014**, *4*, 3381.
[25] Pichaikaran, S.; Arumugam, P. *Green Chem.* **2016**, *18*, 2888.
[26] Pichaikaran, S.; Pandurangan, A. *New J. Chem.* **2017**, *41*, 7893.
[27] Yang, F.; Liu, D.; Wang, H.; Liu, X.; Han, J.; Ge, Q.; Zhu, X. *J. Catal.* **2017**, *349*, 84.
[28] Wang, H.; Ruan, H.; Feng, M.; Qin, Y.; Job, H.; Luo, L.; Wang, C.; Engelhard, M. H.; Kuhn, E.; Chen, X.; Tucker, M. P.; Yang, B. *Chemsuschem* **2017**, *10*, 1846.
[29] Wei, Z; Mao, S; Sun, F; Wang, J; Mei, B; Chen, Y; Li, H; Wang, Y. *Green Chem.* **2018**, *20*, 671.
[30] Zhang, Z.; Wang, F.; Chen, C.; Zhang, T.; Jiang, X.; Yun, Z. *RSC Adv.* **2014**, *4*, 45088.
[31] Hong, Y.-K.; Lee, D.-W.; Eom, H.-J.; Lee, K.-Y. *Appl. Catal. B* **2014**, *150*, 438.
[32] Kokane, R. S.; Acham, V. R.; Kulal, A. B.; Kemnitz, E.; Dongare, M. K.; Umbarkar, S. B. *Chemistryselect* **2017**, *2*, 10618.
[33] Sreekanth, P; Smirniotis, P. *Catal. Lett.* **2008**, *122*, 37.
[34] Meng, M; Guo, L; He, J; Lai, Y; Li, Z; Li, X. *Catal. Today* **2011**, *175*, 72.
[35] Tang, M.; Deng, J.; Li, M.; Li, X.; Li, H.; Chen, Z.; Wang, Y. *Green Chem.* **2016**, *18*, 6082.
[36] Chary, K. V. R.; Srikanth, C. S. *Catal. Lett.* **2008**, *128*, 164.
[37] Jiang, T.; Zhou, Y.; Liang, S.; Liu, H.; Han, B. *Green Chem.* **2009**, *11*, 1000.

[37] Kresse, G.; Furthmuller, J. *Comp. Mater. Sci.* **1996**, *6*, 15.
[39] Kresse, G.; Furthmuller, J. *Phys. Rev. B* **1996**, *54*, 11169.
[40] Blöchl, P. E. *Phys. Rev. B* **1994**, *50*, 17953.
[41] Kresse, G.; Joubert, D. *Phys. Rev. B* **1999**, *59*, 1758.
[42] Hammer, B.; Hansen, L. B.; Norskov, J. K. *Phys. Rev. B* **1999**, *59*, 7413.
[43] Henkelman, G.; Uberuaga, B. P.; Jónsson, H. *J. Chem. Phys.* **2000**, *113*, 9901.

(The following will be filled in by the editorial staff)
Manuscript received: XXXX, 2017
Revised manuscript received: XXXX, 2017
Accepted manuscript online: XXXX, 2017
Version of record online: XXXX, 2017

Entry for the Table of Contents

Page No.

Title **Insight into the Role of Additives in Catalytic Synthesis of Cyclohexylamine from Nitrobenzene**

Xuefeng Li‡, Zhe Wang‡, Shanjun Mao*, Yiqing Chen, Minghui Tang, Haoran Li, Yong Wang*

Max. Table height 6 cm

Text for Table of Contents.